Title	Dynamics of Urban Density in China: Estimations Based on DMSP/OLS Nighttime Light Data
Author(s)	Wu, J; Ma, L; Li, W; Peng, J; Liu, H
Citation	IEEE Journal of Selected Topics in Applied Earth Observations and Remote Sensing, 2014, v. 7 n. 10, p. 4266-4275
Issued Date	2014
URL	http://hdl.handle.net/10722/212323
Rights	IEEE Journal of Selected Topics in Applied Earth Observations and Remote Sensing. Copyright © Institute of Electrical and Electronics Engineers.

Dynamics of Urban Density in China: Estimations Based on DMSP/OLS Nighttime Light Data

Jiansheng Wu, Lin Ma, Weifeng Li, Jian Peng, and Hao Liu

***Abstract*—In China, rapid urbanization has increased the demand for urban land and intensified the conflict between limited land resources and urban development. In response, high urban density has been proposed to realize sustainable urban development. Achieving this goal requires an examination of the dynamics of urban density in China. Nighttime light (NTL) data from the Defense Meteorological Satellite Program/Operational Linescan System (DMSP/OLS) are a good indicator of human activity. We applied NTL data to measure urban density in 70 major cities in China during 1992–2010. Based on temporal changes in NTL, we identified seven classes of urban density and clustered the distributions of urban density in 70 cities into six types. The dynamics of urban density were then obtained from the GDP density as an index of city development. The curves of urban density distribution gradually changed from a concave increase to W-shaped and S-shaped to a concave decrease, indicating that the current urban land use in China is unsustainable and that the shortage of land resources must be addressed. An examination of the distribution of urban density in Hong Kong revealed a different pattern and a potential solution for cities in mainland China.**

***Index Terms*—China, Defense Meteorological Satellite Program/Operational Linescan System (DMSP/OLS), night light, urban density, urbanization.**

I. Introduction

URBANIZATION emerges when many people move from rural areas to urban areas [1]. The boom in urban dwellers leads directly to an increasing demand for urban land to provide housing, infrastructure and services to new migrants as well as improve the living standards of existing habitants [2]. Currently, this demand is mostly satisfied at the expense of converting agricultural land, forests, grassland, wetlands, and open space, which has increased dramatically in recent years and is expected to continue in the coming decades [3]. However, if green fields and arable land are continuously converted into urban land regardless of future needs, environmental problems are inevitable [4], [5]. Urban sprawl breaks up what is left into small portions that disrupt ecosystems and fragment habitats, and causes air pollution since the car-dependent lifestyle imposed by sprawl leads to increases in fossil fuel consumption and emission of greenhouse gases [6], [7]. Many researchers also believe that worldwide urbanization and the impact of human settlements are two of the main causes of global environmental degradation such as habitat loss and alteration, plant and animal species extinction, and ecosystem disruption [8]–[10].

The conflict between urban expansion and environmental protection is more serious in developing countries since the population shift there is large and severe. China, e.g., has been in rapid economic development and urbanization since the early 1980s [11]. The population living in urban areas was less than 20% of the entire nation at that time, while today the proportion is approximately 50%. The fast growth of urban population brings rapid urban land expansion and massive urban housing and infrastructure investment, which is accompanied by substantive conversion of green-fields and prime agricultural land into industrial and residential use [12]. The United Nations predicted that the percentage of urban residents was expected to be 60% by 2020, and the urban population would increase 350 million by 2025 with 219 cities having a population of more than 1 million (compared to 35 cities in Europe) [13].

As China has one-fifth of the world's population, its urbanization has a significant impact on global development. Thus the interests in studying its urban development are growing, and there is an urgent need for China to manage urban land. This study highlights the utility of the Defense Meteorological Satellite Program/Operational Linescan System (DMSP/OLS) nighttime light (NTL) data to analyze the dynamics of urban density in China during 1992–2010.

II. Literature Review

Urban density is mostly characterized by three indices. First is population, such as inhabitant density [14] and employment density [15]. Second is construction like housing density [16] and road network density [17]. Third is the combination of these two indices, e.g., the ratio of the number of high-rise buildings or skyscrapers and the city's population [18], and a three-dimensional matrix consisting of road network density, floor space index (building intensity), and ground space index (building coverage) [17]. Since none of the above indices can be used in a long time series study considering the availability of data, we applied the DMSP/OLS NTL data to analyze the dynamics of urban density in China.

The OLS sensor is part of the U.S. Air Force DMSP [19]. With a swath width of 3000 km, each OLS instrument can

Manuscript received July 08, 2013; revised October 05, 2014; accepted October 27, 2014. Date of publication November 19, 2014; date of current version December 22, 2014. This work was supported in part by National Natural Science Foundation of China under Grant 41271101.

J. Wu and L. Ma are with the Key Laboratory of Human Environmental Science and Technology, Shenzhen Graduate School, Peking University, Shenzhen 518055, China, and also with the College of Urban and Environmental, Peking University, Beijing 100871, China (e-mail: wujs@pkusz.edu.cn; linma2007@hotmail.com).

W. Li is with the Department of Urban Planning and Design, The University of Hong Kong, Hong Kong, China (e-mail: liw.mit@gmail.com).

J. Peng is with the College of Urban and Environmental, Peking University, Beijing 100871, China (e-mail: jianpeng@urban.pku.edu.cn).

H. Liu is with the School of Government, Peking University, Beijing 100871, China (e-mail: liuhao4680@126.com).

Color versions of one or more of the figures in this paper are available online at http://ieeexplore.ieee.org.

Digital Object Identifier 10.1109/JSTARS.2014.2367131

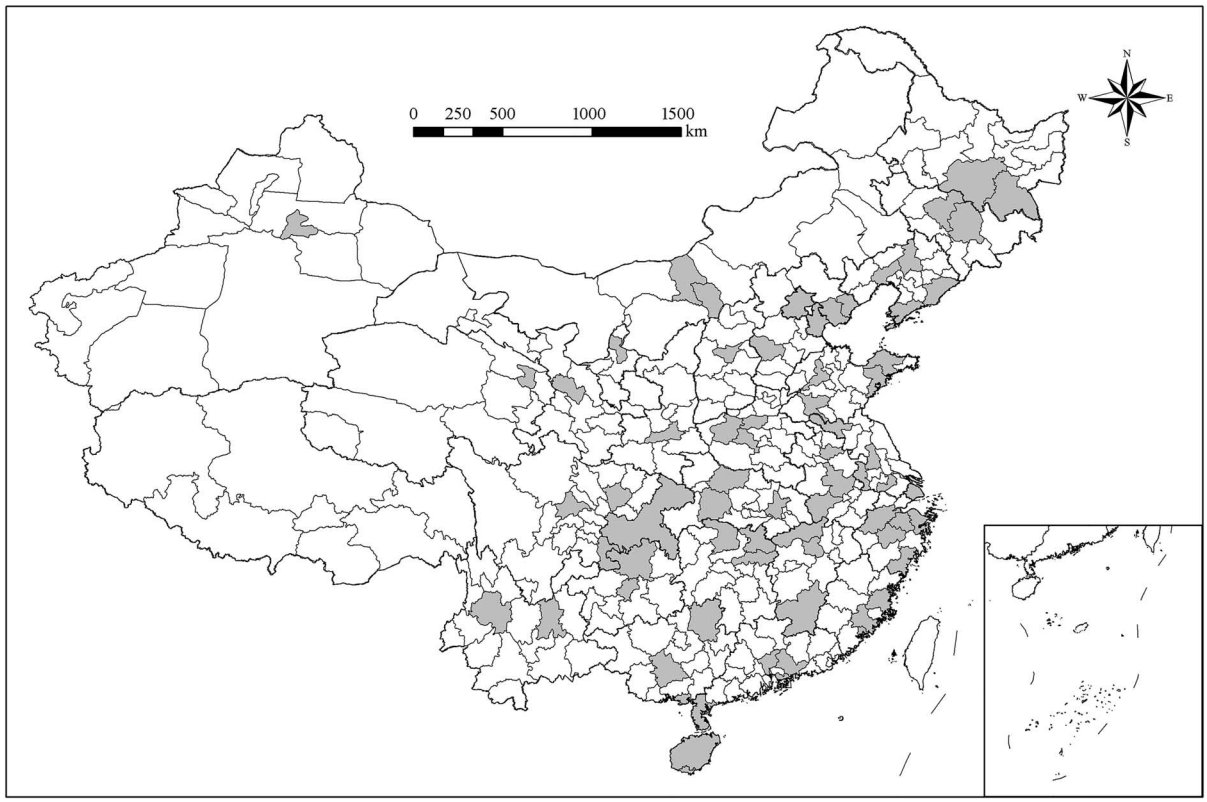

Fig. 1. Locations of 70 cities in China.

collect a complete set of images of earth twice a day [20]. As NTL data have a resolution of 30 arc seconds, which is approximately a square kilometer at the equator, the data can be applied in regional research. The satellite data are initially used to produce nighttime cloud imagery, and the low light-sensing capabilities of the OLS at night allow radiances to be measured down to 10^{-9} $\mathrm{W/cm^2/sr}$ [21]. Due to this high level of sensitivity, the OLS has a unique capability for global mapping artificial lighting present at earth's surface, such as that generated by human settlements, gas flares, fires, and fishing boats [22]. NTL data have been made since 1992, and each grid of the data has a digital number (DN), ranging from 0 to 63, which indicates the annual average NTL intensity [23].

Since the potential of NTL data as an indicator of human activity was identified [24], many studies have been conducted about the relationship between NTL data and key socioeconomic variables, for instance, economic activity [25]–[27], electricity consumption [28], [29], carbon emission [30], [31], and gross domestic product (GDP) [32]–[34]. In particular, population distribution and density has been a topic of interest [35]–[41], and many studies have been conducted in China [42]–[45]. Different from previous studies that focused on urban density in a short duration, our study aims to examine the dynamics of urban density over the past 19 years by using the DMSP/OLS data.

III. Study Area

The study was conducted in 70 major cities in China including many provincial capitals and relatively populous cities (Fig. 1). At the end of 2009, these cities had 34.06% of the nation's population and 65.07% of the GDP (excluding Hong Kong, Macao, and Taiwan) [46]. Therefore, these cities can represent the urban development in China.

IV. Testing the Ability of DMSP/OLS NTL Data to Map Urban Density

There are two issues need to be considered in the application of NTL data. One is the "overglow" effect, which can be described as dim lighting detected from lights in surrounding areas through the scattering of lights in the atmosphere. Townsend and Bruce [28] developed an overglow removal model (ORM) to overcome the effect that based on the relationship between light source strength and the "overglow" distance from the light source to return the light to its source. The ORM functions well in coastal cities such as Melbourne and Sydney in Australia since there are no adjacent light sources to influence the approach. However, most cities in this study are inland, so the distance from the light source is difficult to identify. In reviewing previous studies [47], [48], the threshold method was applied to reduce the effects of "overglow." The pixels with $\mathrm{DN} < 12$ were excluded from analysis.

The other issue is the saturation in urban centers, where the NTL might be brighter, but the DN values are all 63. Letu *et al.* [49], [50] developed two kinds of cubic regression models to correct the saturation: one method can only be applied at the regional level, and the other is based on an assumption that saturated areas did not change during the study period. Therefore, neither of these two models can be used in the research that

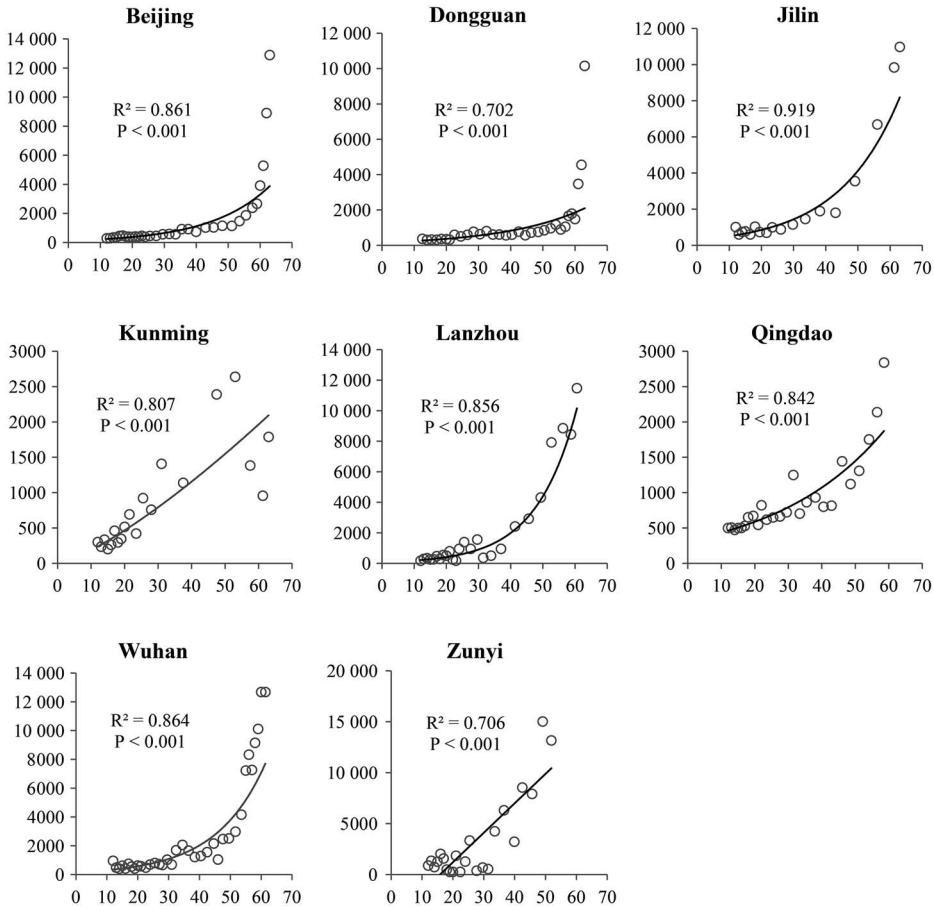

Fig. 2. Test results of population density and NTL data in 2003. Horizontal axle: population density (population per square kilometer) and vertical axle: NTL DN.

focuses on the study at the pixel level in China, a developing country with rapid urban expansion. Based on the rationale that key urban features are inversely correlated with vegetation health and abundance, the Human Settlement Index [51] and the Vegetation Adjusted NTL Urban Index [52] were developed to reduce saturation, which combined MODIS NDVI and NTL. But MODIS NDVI is not available before 2000, which cannot be used to correct saturation for all data in the study period. Consequently, it might need further study to develop a method applicable at the pixel level for long time series. On the other hand, since a major part of this study is the classification of NTL data based on their DN, the saturated area would be identified as urban centers with high values even without correction. Therefore, the saturation would cause no significant bias to the final results, and we think it is acceptable to use NTL data without saturation correction.

It should be noted that when satellites or sensors age and are no longer able to produce data, a replacement satellite is deployed to ensure continuity. Thus, in some years, two satellites collect data and two separate composites are produced. Due to sensor degradation and the difference between the satellites, NTL data collected by two sensors could be different even when there are no real changes on the ground. Therefore, the multitemporal NTL data must be calibrated before the test. Furthermore, there is no onboard calibration on OLS, thus calibration is necessary to ensure that the data of different years or different satellites are comparable. The intercalibration method proposed by Elvidge *et al.* [20] was applied in this research, where the image produced by satellite F12 in 1999 of Sicily is taken as the base reference since the whole image has the wildest spread of DN values, which means satellite F12 in 1999 is able to observe evidence of changes of DN values, and the light in Sicily changes very little over time, so the data from other satellites in other years are adjusted to match the F121999 data range. After intercalibration, if two images were made in 1 year, their mean value was used.

In this research, urban density is characterized by population density, if significant correlations exist between population density and NTL data, the NTL can be used to map urban density. The data of population density are the $1\,\mathrm{km}^2$ grid maps in 1995, 2000, and 2003, provided by the Data Sharing Infrastructure of Earth System Science, so the NTL images in 1995, 2000, and 2003 are used. First, eight cities were chosen as testing area, including Beijing, Dongguan, Jilin, Kunming, Lanzhou, Qingdao, Wuhan, and Zunyi. Next the NTL data were divided into 20–30 categories based on the DN values. We then analyzed the population density and the mean DN value in each category by using the Statistical Package for the Social Sciences (SPSS).

The results (due to space constraints, only the results in 2003 were shown in Fig. 2) imply that the NTL data are associated with population density through several positive monotonic functions [47], and therefore they can be applied to map urban density in this study.

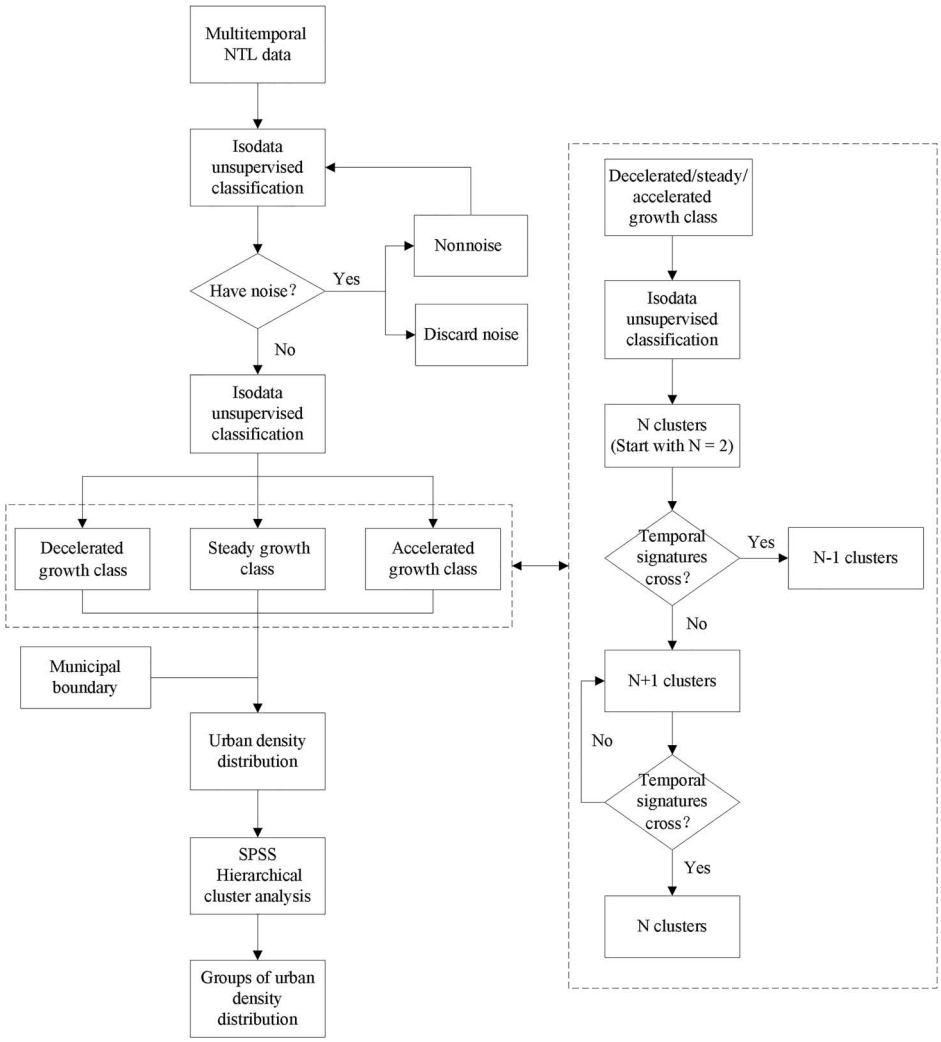

Fig. 3. Flowchart showing major steps to map urban density distribution using multitemporal NTL images.

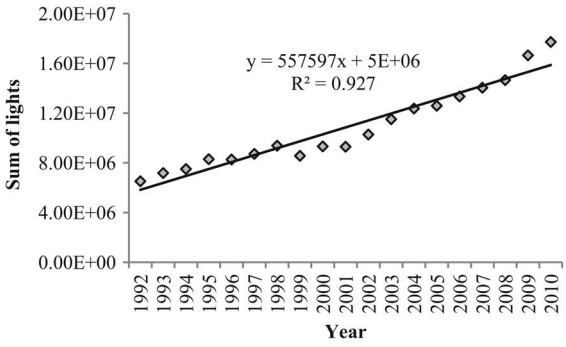

Fig. 4. Sum of light in China during 1992–2010.

We also noticed that the maximum of population density in these cities are different. The reasons may be that each city has its specific history, culture, citizens' living habits, and natural environments such as topography and climate. Furthermore, because we conducted the study in the urban areas of the most developed cities in China, the land use conditions are similar. So, we believe the urban density in these cities is comparable.

TABLE I
INPUT DMSP/OLS NTL DATA FROM 1992 TO 2010

Year	Satellite					
1992	F10					
1995		F12				
1998		F12	F14			
2001			F14	F15		
2004				F15	F16	
2007				F15	F16	
2010						F18

V. METHODOLOGY

The analysis consists of two steps and is summarized in Fig. 3.

A. Classification of Multitemporal NTL Data Using Iterative Isodata Clustering Algorithm

Since the lighting in China steady grows during 1992–2010 (Fig. 4) [32]–[34], we used NTL images at 3-year intervals as input (Table I) to simplify the data processing. An iterative unsupervised classification that used Isodata clustering

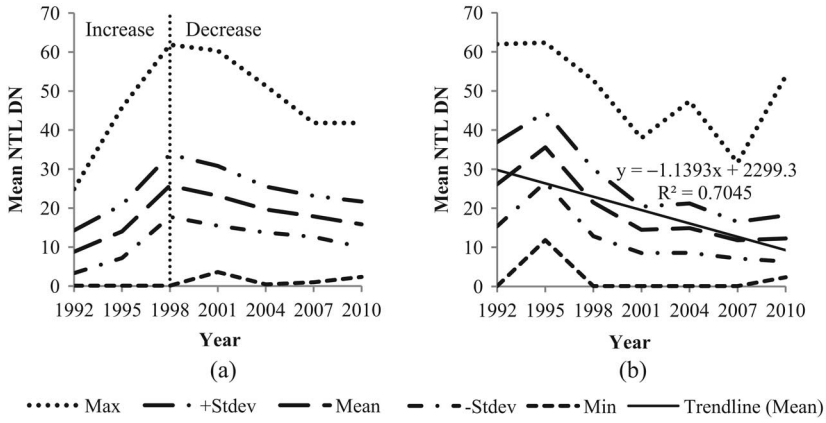

Fig. 5. Representative temporal signatures of noises: (a) with a trend of decrease and (b) with a duration of decrease equal to or longer than half of the entire period.

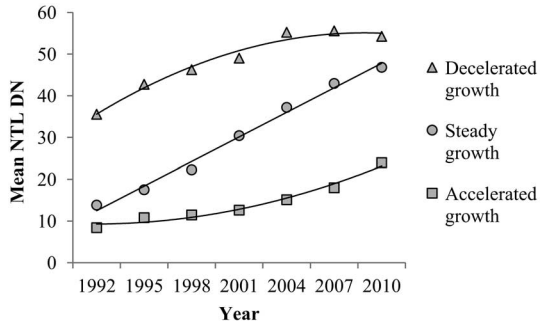

Fig. 6. Temporal signatures of three basic urbanization trajectories.

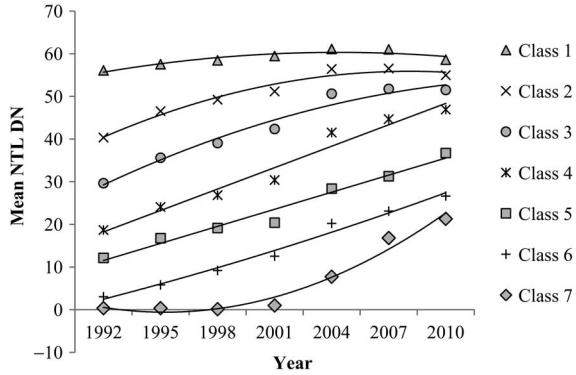

Fig. 7. Temporal signatures of the final classification.

algorithm [51], [53] was applied to classify the multitemporal NTL data. The iterative technique involved removing noise after each classification and classifying the remaining NTL data based on the DN value. First, the clusters with $\mathrm{DN} < 12$ in the entire period were removed to reduce "overglow" effects. As the lighting in China keeps growing in recent years, the clusters with temporal signatures against this general trend were identified as noise, which assumed to be caused by system bias and not included in further analysis. Since there was no region remaining constant during 1992–2010 in the study area, the noise was defined as those whose temporal signatures had a trend of decrease [Fig. 5(a)] or a duration of decrease equal to or longer than half of the entire period [Fig. 5(b)].

After removing the noise, we first divided the remaining data into three basic clusters based on the urbanization trajectories around the world (Fig. 6). The temporal signature of the decelerated growth class is a convex shape, which indicates a fast development in early years. Regions with a high level of urbanization such as urban cores are supposed to be in this class. In contrast, the accelerated growth class represents regions that develop fast in recent years, so its temporal signature has a concave shape. The steady growth class is the region where urban population and economy exhibit much change, so its signature tends to be a straight line. Considering the rapid urbanization in China, the de-urbanization, which has a decline in urban population, is not considered.

To further analyze the temporal changes of NTL data under the general trend of urbanization, we then subdivided these three clusters. Apparently, dividing the data into many clusters would reveal detail information about urban density, but make multitemporal signatures complex and difficult to analyze. Thus, a proper number of clusters are necessary. Our method was to subdivide each of the three clusters on the premise that their multitemporal signatures do not cross, on which we would have a further discussion later in this paper.

B. Classification of Urban Density Distribution Using SPSS

After classification of multitemporal NTL data, the municipal boundary was overlaid to get the classification results in each city. Assuming the multitemporal NTL images are divided into M clusters, the classification results in each city can be characterized in the form of a ratio

$$\mathrm{Ratio_I} = \frac{\mathrm{N_I}}{\mathrm{N_S}} \times 100\% \tag{1}$$

where $\mathrm{N_I}$ is the area of a particular NTL cluster, $\mathrm{I} = 1, 2, \ldots, \mathrm{M}$ and $\mathrm{N_S}$ is the sum of $\mathrm{N_I}$.

The distribution of urban density in the 70 cities can be presented in the form of an M-dimensional array

$$\text{Urban Density Distribution}_\mathrm{j} = (\mathrm{Ratio_1}, \mathrm{Ratio_2}, \ldots, \mathrm{Ratio_M}) \tag{2}$$

where $\mathrm{j} = 1, 2, \ldots, 70$.

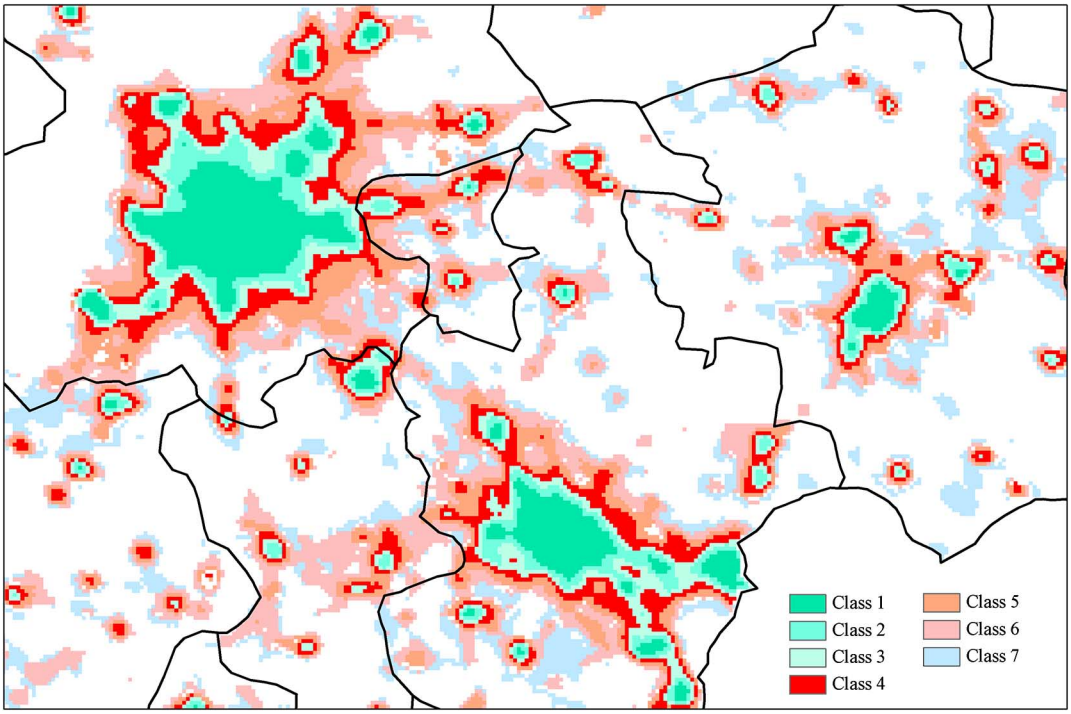

Fig. 8. Final classification man in Beijing–Tianjin–Hebei region.

TABLE II
URBAN DENSITY DISTRIBUTION IN SHENZHEN, BEIJING, WUHAN, AND TANGSHAN

	City	Class 1	Class 2	Class 3	Class 4	Class 5	Class 6	Class 7	Sum
Number of lighting pixels	Shenzhen	832	352	221	197	126	41	9	1778
	Beijing	1167	634	626	1003	1331	1358	389	6508
	Wuhan	257	230	206	432	454	361	744	2684
	Tangshan	115	124	186	409	582	823	1452	3691
Ratio (%)	Shenzhen	46.79	19.80	12.43	11.08	7.09	2.31	0.51	100.00
	Beijing	17.93	9.74	9.62	15.41	20.45	20.87	5.98	100.00
	Wuhan	11.85	7.10	7.63	14.87	17.27	15.89	25.39	100.00
	Tangshan	3.12	3.36	5.04	11.08	15.77	22.30	39.34	100.00

We then used the hierarchical cluster analysis based within-groups linkage of the SPSS to cluster cities that had similar distribution of urban density, since it can better distinguish the difference between cities.

VI. RESULTS

The multitemporal NTL data are classified into seven types (Fig. 7). A final classification map for part of Beijing–Tianjin–Hebei is shown in Fig. 8. The green regions (Class 1–Class 3) have highest DN values and convex-shaped temporal signatures, which are likely to be urban cores with high urban density. The DN values in red regions (Class 4–Class 6) grow rapidly in the study period and their temporal signatures are straight lines. The blue regions are Class 7; its concave shaped curve indicates a fast growth in recent years.

The distribution of urban density in the 70 cities was then calculated, part of which was shown in Table II. Through SPSS clustering analysis, the 70 cities are divided into six groups (Fig. 9). There are 9, 14, 17, and 26 cities in Groups A, B, C, and D, respectively. Group E has three cities: Shanghai, Beijing, and Guangzhou, and only Shenzhen is in Group F.

VII. DISCUSSION

A. Dynamics of Urban Density Based on GDP Density

As an important indicator of city development, GDP was applied to obtain the dynamics of urban density. To reduce the influence of city area (if two cities are in the same level of development, the city with larger area would have higher GDP), the GDP density was used, which was defined as

$$\text{GDP density} = \frac{G_2 + G_3}{A} \tag{3}$$

where G_2 and G_3 are the GDP of secondary industry and tertiary industry. Since primary industry including agriculture, forestry, and fishing rarely occurs in urban area, the GDP of primary industry is not considered. A is the area of a particular city, which is recorded in the China city statistical yearbook.

Based on the assumption that developed cities have higher GDP density than developing cites, we ranked the 70 cities based on their GDP density and explored the relationship between urban density and city development. Fig. 10 shows the

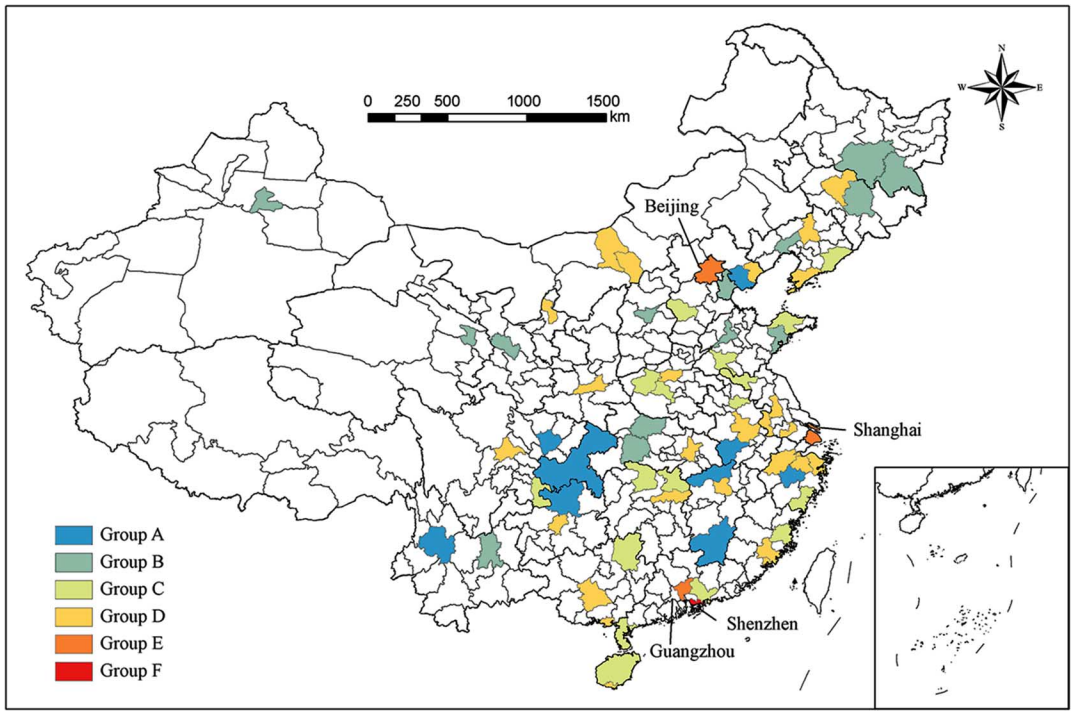

Fig. 9. Six groups of cities through SPSS analysis.

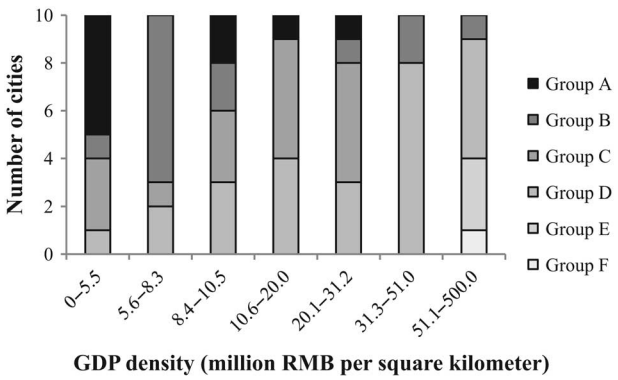

Fig. 10. Seventy cities ranked by GDP density in the group of 10 cities.

rank in the group of 10 cities. In the lowest level of GDP density, which represents the primary stage of development, most cities are in Group A. The major kind of each group gradually changes to Group B, Group C, and Group D as GDP density grows, which implies that the distribution of urban density changes with development. Both Group E and Group F are in the highest level of GDP density, so they are likely to be the most developed cities.

Based on this trend, we calculated the average distribution of each city group to further analysis the dynamics (Fig. 11). As the only city in Group F, Shenzhen has seen rapid economic growth since it became a special economic zone in 1979. In the last 19 years, the annual growth of GDP and population in Shenzhen are as high as 21.79% and 7.61%, respectively. However, along with the soaring development, large amount of land resources have been used. According to the "Urban Planning of Shenzhen (2010–2020)," the unused land area is predicted to be only $26.36\,\mathrm{km}^2$ in 2020, which is only 1.35% of the total land area. The land resource shortage has become a serious problem of city development.

There are three cities in Group E. Since their population density and GDP density are lower than that of Shenzhen, we consider them as the second most developed cities. The curve of urban density distribution (Fig. 11) shows that the area with decelerated growth and steady growth is equal to more than 90% of the total area, thus the urban density in Group E may become similar to that of Group F without future control measures. Taking Guangzhou and Shanghai as examples, according to the China City Statistical Yearbook [46], [54], the population in Guangzhou and Shanghai in 2010 increased by 170% compared with 1992. The population growth would bring huge demand for urban facilities and land and lead to the rise in urban density.

The GDP density and urban population density of Group B, Group C, and Group D are all higher than that of Group A and lower than that of Group E. Since the difference between their GDP density and urban population density was small, it is difficult to measure the development between them, so we consider them to be in a same period of development but with different trajectories.

The distribution of urban density of Group A is opposite to that of Group F, and since these cities have lowest GDP density and urban population density, we believe that Group A is in the primary period of city development.

B. Is There a Better Pattern for Chinese Urban Land Use?

The dynamics of urban density indicate that much land has been densely used in the last 19 years, and the problem of land resource shortage is serious as cities develop and hold more people. Though only Shenzhen is in Group F, we believe that

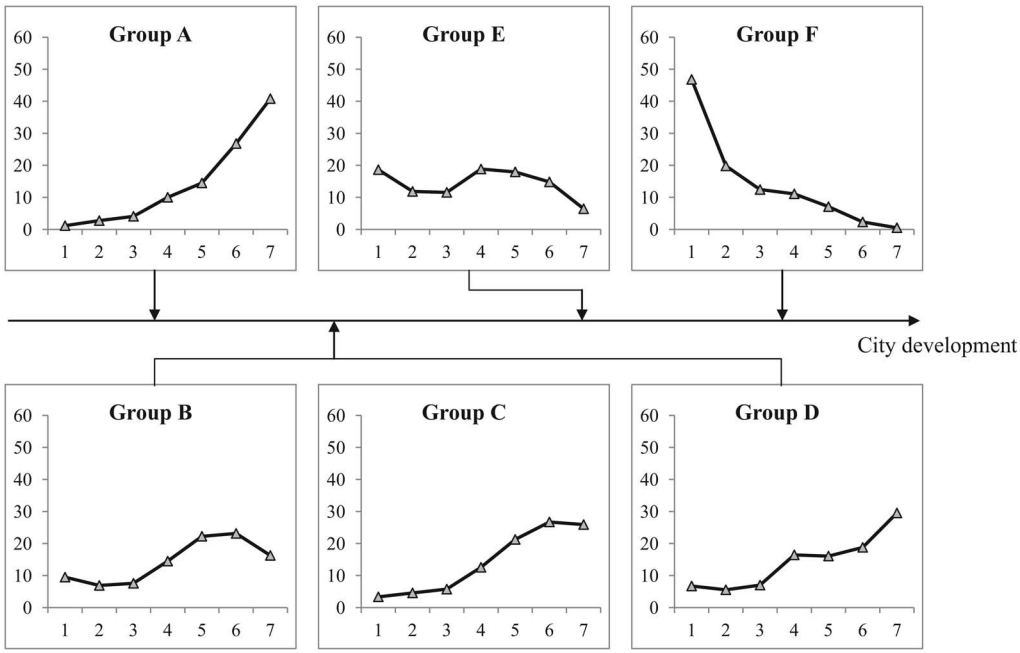

Fig. 11. Dynamics of urban density with city development. Horizontal axle: Class of multitemporal NTL data and vertical axle: Ratio of area (%).

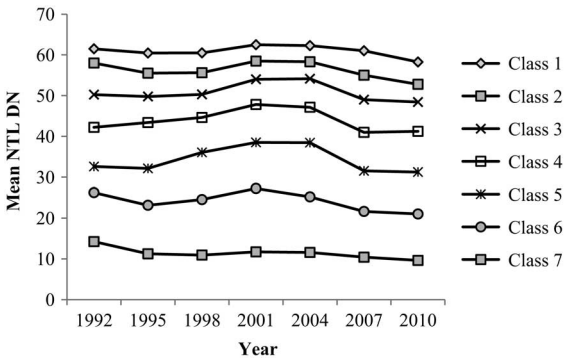

Fig. 12. Temporal signatures of Hong Kong.

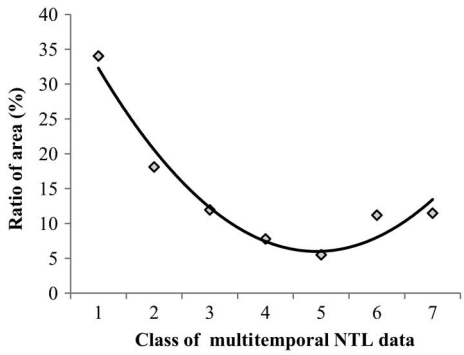

Fig. 13. Curve of urban density distribution in Hong Kong.

the current urban land use in China is unsustainable without controlling method.

The political, economic, and cultural environments in Hong Kong are different from cities in mainland China, so it is not included in the study. However, we found that Hong Kong had approximately 7 097 600 people at the end of 2010 [55] and its entire area was merely $1108\,\mathrm{km}^2$ [56]. Furthermore, its GDP density was 15.78×10^8 Hong Kong dollars (about 12.62×10^8 Chinese Yuan) per square kilometer [57], which means the land in Hong Kong has higher urban density than all 70 cities in this research.

To consistent with the previous analysis, the multitemporal NTL data in Hong Kong during 1992–2010 were classified into seven clusters using the same method. Different from mainland cities, the urban density in Hong Kong is stable (Fig. 12) and the distribution curve shows an "U" shape (Fig. 13), which indicates that the major part of the urban land is with high density like the cities in Group E and Group F, but more than 10% of the total land has low density. Compared with Group E and Group F, we believe that the "U" shape is a better pattern for urban land use and urban density distribution, since it has both high urban density area, which caused by population gathering and city development, and a certain amount of land as reserved resource, which is essential for sustainable development.

C. NTL Data Saturation and Classification

Since the classification of urban density is based on the DN value, the saturation of NTL data does not largely affect the recognition of urban centers and the classification of urban density distribution after. Since there is no correction method applicable in long time series study at the pixel level, the saturation effect is not considered in this study. However, to get more accurate discoveries, the saturation correction is still needed.

In the classification process, we divided the multitemporal NTL data into seven clusters. If the data were classified into different number of clusters, their temporal signatures would also change. Fig. 14 shows the results of four clusters and ten clusters. It is obvious that more clusters would have more complex temporal signatures, but they all match with the general urbanization trajectories. To clearly recognize and further compare different temporal changes of DN values, we classified the data

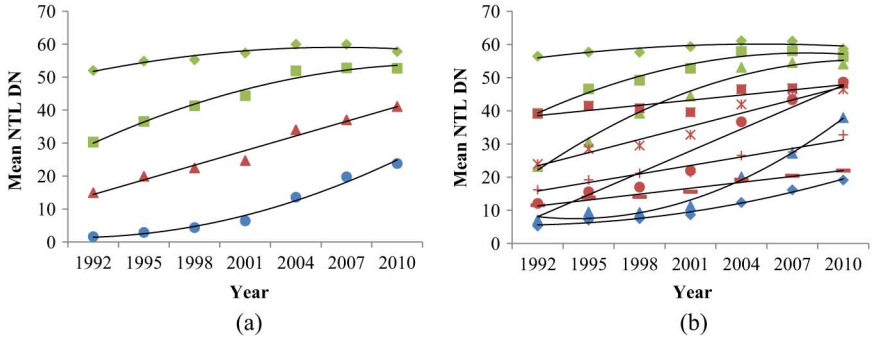

Fig. 14. Temporal signatures of different classification: (a) four clusters and (b) ten clusters.

into seven clusters and got the "parallel" temporal signatures (Fig. 7), which shows the trend of urbanization and is easy to analyze at the same time.

VIII. Conclusion

Multitemporal DMSP/OLS data can be used to map urban density in China at city level. Urban regions with higher population density tend to have higher NTL brightness. By dividing the multitemporal NTL data based on temporal changes in NTL brightness, our results verified the ability of DMSP/OLS night lights for reflecting three basic urbanization trajectories: decelerated growth, steady growth, and accelerated growth. Moreover, our analysis revealed six kinds of urban density distributions in 70 major cities in mainland China, which fall into four categories: concave increase, W-shaped, S-shaped, and concave decrease. As city gathering more people and GDP, the urban density distribution tends to change from concave increase through W-shaped and S-shaped to concave decrease. Though part of the process is not clear, we believe that by integrating more socioeconomic variables and analysis, more discoveries can be made about the dynamics of urban density. The dynamics of urban density indicated that the overall urban land use in China is unsustainable and the shortage of land resources must be addressed. Furthermore, we analyzed the urban density in Hong Kong and considered it as a better pattern for city development since there was a certain amount of land with low urban density kept as reserved resources under its general high urban density.

In addition, there are two challenges for applications of DMSP/OLS data in assessment of local scale urbanization processes: the saturation in bright cores of urban centers and "overglow" effect. Therefore, further studies on correction methods applicable at the pixel level and for long time series are needed.

Acknowledgment

The authors would like to thank three anonymous reviewers for their constructive remarks.

References

[1] X. L. Zhang *et al.*, "An evaluation framework for the sustainability of urban land use: A study of capital cities and municipalities in China," *Habitat Int.*, vol. 35, pp. 141–149, Jan. 2011.

[2] M. H. Tan *et al.*, "Urban land expansion and arable land loss in China—A case study of Beijing–Tianjin–Hebei region," *Land Use Policy*, vol. 22, pp. 187–196, Jul. 2005.

[3] United Nations, *World Urbanization Prospects—The 2007 Revision*, United Nations, New York, NY, USA, 2008.

[4] G. Dally and M. Power, "Nature's services: Societal dependence on natural ecosystems," *Nature*, vol. 388, p. 529, 1997.

[5] Millennium Ecosystem Assessment, *Ecosystems and Human Well-Being: A Framework for Assessment.* Washington, DC, USA: Island Press, 2003.

[6] E. H. Wilson *et al.*, "Development of a geospatial model to quantify, describe and map urban growth," *Remote Sens. Environ.*, vol. 86, pp. 275–285, Aug 2003.

[7] Q. A. Zhang *et al.*, "Simulation and analysis of urban growth scenarios for the Greater Shanghai Area, China," *Comput. Environ. Urban Syst.*, vol. 35, pp. 126–139, Mar. 2011.

[8] E. Shochat *et al.*, "From patterns to emerging processes in mechanistic urban ecology," *Trends Ecol. Evol.*, vol. 21, pp. 186–191, Apr. 2006.

[9] R. I. McDonald *et al.*, "The implications of current and future urbanization for global protected areas and biodiversity conservation," *Biol. Conserv.*, vol. 141, pp. 1695–1703, Jun. 2008.

[10] Y. Ban and O. A. Yousif, "Multitemporal spaceborne SAR data for urban change detection in China," *IEEE J Sel. Topics Appl. Earth Observ. Remote Sens.*, vol. 5, no. 4, pp. 1087–1094, Aug. 2012.

[11] J. Y. Liu *et al.*, "Land-cover classification of China: Integrated analysis of AVHRR imagery and geophysical data," *Int. J. Remote Sens.*, vol. 24, pp. 2485–2500, Jun. 20, 2003.

[12] D. Rousseau and Y. Chen, "Sustainability options for China's residential building sector," *Build. Res. Inf.*, vol. 29, pp. 293–301, Jul 2001.

[13] United Nations. *World Population Prospects—The 2010 Revision*, United Nations, New York, NY, USA, 2011.

[14] N. Karathodorou *et al.*, "Estimating the effect of urban density on fuel demand," *Energy Econ.*, vol. 32, pp. 86–92, Jan 2010.

[15] G. A. Carlino *et al.*, "Urban density and the rate of invention," *J. Urban Econ.*, vol. 61, pp. 389–419, May 2007.

[16] A. M. Coutts *et al.*, "Impact of increasing urban density on local climate: Spatial and temporal variations in the surface energy balance in Melbourne, Australia," *J. Appl. Meteorol. Climat.*, vol. 46, pp. 477–493, Apr. 2007.

[17] E. M. Salomons and M. B. Pont, "Urban traffic noise and the relation to urban density, form, and traffic elasticity," *Landscape Urban Plann.*, vol. 108, pp. 2–16, Oct. 2012.

[18] S. Titman and G. Twite, "Urban density, law and the duration of real estate leases," *J. Urban Econ.*, vol. 74, pp. 99–112, Mar. 2013.

[19] C. D. Elvidge *et al.*, "Mapping city lights with nighttime data from the DMSP operational linescan system," *Photogramm. Eng. Remote Sens.*, vol. 63, pp. 727–734, Jun. 1997.

[20] C. D. Elvidge *et al.*, "A fifteen year record of global natural gas flaring derived from satellite data," *Energy*, vol. 2, pp. 595–622, Sep 2009.

[21] C. D. Elvidge *et al.*, "Overview of DMSP nightime lights and future possibilities," *2009 Joint Urban Remote Sens. Event*, vol. 1–3, pp. 1665–1669, 2009.

[22] C. D. Elvidge *et al.*, "Night-time lights of the world: 1994–1995," *ISPRS J. Photogramm. Remote Sens.*, vol. 56, pp. 81–99, Dec. 2001.

[23] K. Baugh *et al.*, "Development of a 2009 stable lights product using DMSP-OLS data," in *Proc. 30th Meet. Asia–Pacific Adv. Netw.*, vol. 30, pp. 114–130, 2010.

[24] T. A. Croft, "Nighttime images of the earth from space," *Sci. Am.*, vol. 239, pp. 86–98, 1978.

[25] J. V. Henderson *et al.*, "Measuring economic growth from outer space," *Am. Econ. Rev.*, vol. 102, pp. 994–1028, Apr. 2012.

[26] C. N. H. Doll *et al.*, "Mapping regional economic activity from night-time light satellite imagery," *Ecol. Econ.*, vol. 57, pp. 75–92, Apr. 2006.

[27] J. S. Wu *et al.*, "Hierarchical structure and spatial pattern of China's urban system: Evidence from DMSP/OLS nightlight data," *J. Geogr. Sci.*, vol. 69, pp. 759–770, Jun. 2014 (in Chinese).
[28] A. C. Townsend and D. A. Bruce, "The use of night-time lights satellite imagery as a measure of Australia's regional electricity consumption and population distribution," *Int. J. Remote Sens.*, vol. 31, pp. 4459–4480, 2010.
[29] T. R. K. Chand *et al.*, "Spatial characterization of electrical power consumption patterns over India using temporal DMSP-OLS night-time satellite data," *Int. J. Remote Sens.*, vol. 30, pp. 647–661, 2009.
[30] M. R. Raupach *et al.*, "Regional variations in spatial structure of nightlights, population density and fossil-fuel CO2 emissions," *Energy Policy*, vol. 38, pp. 4756–4764, Sep. 2010.
[31] C. N. H. Doll *et al.*, "Night-time imagery as a tool for global mapping of socioeconomic parameters and greenhouse gas emissions," *Ambio*, vol. 29, pp. 157–162, May 2000.
[32] P. C. Sutton *et al.*, "Estimation of gross domestic product at sub-national scales using nighttime satellite imagery," *Int. J. Ecol. Econ. Stat.*, vol. 8, pp. 5–21, 2007.
[33] S. Ebener *et al.*, "From wealth to health: Modelling the distribution of income per capita at the sub-national level using night-time light imagery," *Int. J. Health Geogr.*, vol. 4, p. 5, 2005.
[34] C. D. Elvidge *et al.* (2014). *National Trends in Satellite Observed Lighting: 1992–2012* [Online]. Available: http://ngdc.noaa.gov/eog/dmsp/download_national_trend.html
[35] P. K. R. Chowdhury *et al.*, "Estimation of urban population in Indo-Gangetic Plains using night-time OLS data," *Int. J. Remote Sens.*, vol. 33, pp. 2498–2515, 2012.
[36] S. Amaral *et al.*, "DMSP/OLS night-time light imagery for urban population estimates in the Brazilian Amazon," *Int. J. Remote Sens.*, vol. 27, pp. 855–870, Mar. 2006.
[37] C. D. Elvidge *et al.*, "Relation between satellite observed visible-near infrared emissions, population, economic activity and electric power consumption," *Int. J. Remote Sens.*, vol. 18, pp. 1373–1379, Apr. 1997.
[38] P. Sutton, "Modeling population density with night-time satellite imagery and GIS," *Comput. Environ. Urban Syst.*, vol. 21, pp. 227–244, Jul. 1997.
[39] P. Sutton *et al.*, "A comparison of nighttime satellite imagery and population density for the continental united states," *Photogramm. Eng. Remote Sens.*, vol. 63, pp. 1303–1313, Nov. 1997.
[40] R. Welch, "Monitoring urban-population and energy-utilization patterns from satellite data," *Remote Sens. Environ.*, vol. 9, pp. 1–9, 1980.
[41] P. C. Sutton, "Estimation of human population parameters using night-time satellite imagery," in *Remotely-Sensed Cities*. Boca Raton, FL, USA: CRC Press, 2003, p. 301.
[42] X. Yang *et al.*, "Spatial improvement of human population distribution based on multi-sensor remote-sensing data: an input for exposure assessment," *Int. J. Remote Sens.*, vol. 34, pp. 5569–5583, Aug. 2013.
[43] C. Q. Zeng *et al.*, "Population spatialization in China based on night-time imagery and land use data," *Int. J. Remote Sens.*, vol. 32, pp. 9599–9620, 2011.
[44] C. P. Lo, "Modeling the population of China using DMSP operational linescan system nighttime data," *Photogramm. Eng. Remote Sens.*, vol. 67, pp. 1037–1047, Sep. 2001.
[45] L. Zhuo *et al.*, "Modelling the population density of China at the pixel level based on DMSP/OLS non-radiance-calibrated night-time light images," *Int. J. Remote Sens.*, vol. 30, pp. 1003–1018, 2009.
[46] National Bureau of Statistics of China, *China City Statistical Yearbook—The 2010 Revision*, China Statistics Press, Beijing, China, 2011.
[47] T. Ma *et al.*, "Quantitative estimation of urbanization dynamics using time series of DMSP/OLS nighttime light data: A comparative case study from China's cities," *Remote Sens. Environ.*, vol. 124, pp. 99–107, Sep. 2012.
[48] C. Small *et al.*, "Spatial scaling of stable night lights," *Remote Sens. Environ.*, vol. 115, pp. 269–280, Feb. 2011.
[49] H. Letu *et al.*, "A saturated light correction method for DMSP/OLS night-time satellite imagery," *IEEE Trans. Geosci. Remote Sens.*, vol. 50, no. 2, pp. 389–396, Feb. 2012.
[50] H. Letu *et al.*, "Estimating energy consumption from night-time DMPS/OLS imagery after correcting for saturation effects," *Int. J. Remote Sens.*, vol. 31, pp. 4443–4458, 2010.
[51] D. S. Lu *et al.*, "Regional mapping of human settlements in southeastern China with multisensor remotely sensed data," *Remote Sens. Environ.*, vol. 112, pp. 3668–3679, Sep. 2008.
[52] Q. Zhang *et al.*, "The vegetation adjusted NTL urban index: A new approach to reduce saturation and increase variation in nighttime luminosity," *Remote Sens. Environ.*, vol. 129, pp. 32–41, Feb. 2013.
[53] Q. L. Zhang and K. C. Seto, "Mapping urbanization dynamics at regional and global scales using multi-temporal DMSP/OLS nighttime light data," *Remote Sens. Environ.*, vol. 115, pp. 2320–2329, Sep. 2011.
[54] National Bureau of Statistics of China, *China City Statistical Yearbook—The 1992 Revision*, China Statistics Press, Beijing, China, 1993.
[55] Census, and Statistics Department. (2012). *Year-End Population for 2010* [Online]. Available: http://www.censtatd.gov.hk/press_release/press_releases_on_statistics/index.jsp?sID=2691&sSUBID=17828&displayMode=D
[56] Census, and Statistics Department. (2012). *Land Utilization in Hong Kong* [Online]. Available: http://www.pland.gov.hk/pland_en/info_serv/statistic/landu.html
[57] Census, and Statistics Department. (2011). *Gross Domestic Product (Yearly) (2010 Edition)*. The Government of the Hong Kong Special Administrative Region [Online]. Available: http://www.censtatd.gov.hk/fd.jsp? file = B10300022010AN10E0100.pdf&product_id=B1030002&lang=1

Jiansheng Wu received the B.S. degree in engineering geology and hydrogeology from the Southwest Jiaotong University, Emei, China, and the M.S. degree in cartography and remote sensing from Peking University, Beijing, China, in 1987 and 1990, respectively, and the Ph.D. degree in cartography and GIS from the Institute of Geographic Sciences and Natural Resources Research, Chinese Academy of Sciences, Beijing, China, in 2001.

He is currently a Professor with Peking University. His research interests include remote sensing, GIS, landscape ecology, and land use.

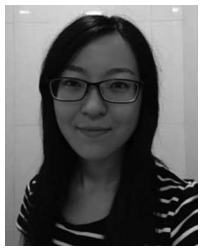

Lin Ma received the B.S. degree in land resources management from China University of Geosciences, Beijing, China, in 2011. Currently, she is pursuing the Ph.D. degree in geography at Peking University, Beijing, China.

Her research interests include land use and landscape ecology.

Weifeng Li received the B.S. and M.S. degrees in geography from Peking University, Beijing, China, in 1997 and 2001, respectively, and the Ph.D. degree in urban and regional planning from Massachusetts Institute of Technology, Cambridge, MA, USA, in 2011.

He is currently an Assistant Professor with the University of Hong Kong, Hong Kong. His research interests include in the areas of environmental sustainability, land use transportation planning interactions and the environmental impacts, as well as the use of GIS, remote sensing, and big data in urban planning.

Jian Peng received the B.S. degree in geography from Beijing Normal University, Beijing, China, and the Ph.D. degree in geography from Peking University, Beijing, China, in 1999 and 2007, respectively.

Currently, he is an Associate Professor with Peking University. His research interests include integrated ecosystem assessment, and landscape ecology and land use.

Hao Liu received the B.S. degree in resource environment and urban planning and management from Central China Normal University, Wuhan, China, in 2011. Currently, he is pursuing the Ph.D. degree in regional economics at Peking University, Beijing, China.

His research interests include urban and regional planning, economic geography, and sustainable development.